Investigations on the Frequency Dependence of the Delay Spread in an UMi Street Canyon Scenario

Michael Peter, Richard J. Weiler, Fabian Undi, Farouk El-Kanawati, Stephan Jaeckel,
Leszek Raschkowski, Lars Thiele, Kei Sakaguchi, and Wilhelm Keusgen
Fraunhofer Heinrich Hertz Institute, Einsteinufer 37, 10551 Berlin, Germany

Abstract - **A channel measurement campaign was carried out in Berlin, Germany, aiming to provide multi-frequency data for the urban microcellular (UMi) access channel in the street canyon. Four bands (10.25, 28.5, 41.5 and 82.5 GHz) were measured simultaneously. In this paper, statistical evaluations on the frequency dependence of the root-mean-square delay spread (DS) under line of sight (LOS) conditions are presented. The largest values occur for 10.25 GHz when a high relative evaluation threshold is used, and the values are smallest for 82.5 GHz. However, a distinct and clear frequency dependence cannot be observed for the measured scenario. The estimated DS is very sensitive to data selection and processing.**

Index Terms — Channel measurements, mm-wave propagation, delay spread, frequency dependence

1. Introduction

Fifth generation (5G) mobile networks will need to make use of much higher frequencies to provide ultra-high data rates and capacity [1]. The targeted frequency bands comprise a huge range up to 100 GHz. Since the provision of an accurate reference channel model is essential for enabling link and system level simulations at these high frequencies, there are strong related activities in the research community and standardization bodies like 3GPP and ITU-R. Most of the work strongly builds upon state-of-the-art three-dimensional (3D) geometry-based stochastic channel models (GSCMs) that have been developed in recent years for the lower frequency bands [2], [3], [4], [5]. The ultimate target is to elaborate a flexible and comprehensive frequency-agile channel model that covers the entire range up to 100 GHz for targeted 5G scenarios rather than providing a model for specific bands only. With this respect, the question arises to what extend the large-scale parameters (LSPs), like DS and the angular spreads, depend on frequency.

2. Channel Sounder Setup

The measurements were carried out with a multi-frequency wideband channel sounder based on dedicated hardware. The schematics and photos are shown in [2]. The sounder consists of four parallel transmit/receive chains, which were used at the carrier frequencies 10.25, 28.5, 41.5 and 82.5 GHz. The same baseband signal with 1.5 GHz bandwidth was feed into the 28, 41 and 82 GHz transmit chains. Due to regulatory reasons, the bandwidth at 10 GHz was limited to 500 MHz. The signal generators periodically repeated a PAPR-optimized 2.56 μs long sounding sequence. A transmit power of 30 dBm could be achieved at 10 and 28 GHz. It was lower for 41 GHz (20 dBm) and 82 GHz (11 dBm). Self-built omnidirectional antennas with vertical polarization at both, the transmitter (Tx) and the receiver (Rx) were used. Synchronization between Tx and Rx is ensured via temperature-controlled rubidium clocks and the system is calibrated on site via back-to-back measurements. At the receiver, the signals are amplified, down-converted, filtered and sampled at IF stage. Real-time averaging (averaging factor of 100) over multiple sequence periods further improves the signal-to-noise ratio of the received signal. Post-processing, e.g. down-conversion to baseband, and further averaging, is performed offline.

3. Measurement Scenario and Procedure

The measurement campaign was performed in a busy shopping street in downtown Berlin, Germany. The uniform street canyon is 2 km long, has a width of approximately 20 m and is bordered by 7–8-storey buildings. The Tx was placed on the sidewalk close to an intersection with 10 m distance from the building corner and at 5 m height. The Rx was mounted on a camera dolly at a height of 1.5 m and moved along the sidewalk on seven measurement tracks with a constant speed of 0.5 m/s. In conjunction with a snapshot separation of 2 ms, this corresponds to a spacing of 1 mm between adjacent channel observations. Three of the tracks were measured in LOS condition. Each started at 10 m distance from the Tx and consisted of six consecutive 50 m segments, adding up to 300 m total track length with a maximum distance of 310 m. Details can be found in [2].

4. Delay Spread Analysis

For each segment of 50 m length, 50,000 channel impulse responses (CIRs) are available. In a first processing step the CIRs were reduced to 500 MHz bandwidth and a Kaiser window (parameter $\beta = 6$) was applied in the frequency domain to reduce the sidelobes in the delay domain. Lowpass-interpolated versions (upsampling factor 4) of the CIRs were used for further processing. The DS was calculated based on averaged power delay profiles (APDPs). Each APDP was obtained by averaging over K successive CIRs according to

$$P(\tau) = \frac{1}{K}\sum_{k=1}^{K} |h_k(\tau)|^2,$$

where $P(\tau)$ denotes the APDP and $h_k(\tau)$ is the k^{th} CIR. An averaging factor of $K = 100$ was used, which corresponds to a spatial averaging over 10 cm. A relative threshold Γ with respect to the maximum in $P(\tau)$ was applied and contributions below the threshold were discarded [6]. Great care has been taken to ensure that the dynamic range of the APDPs was always large enough to support the respective threshold in order to exclude distortions of the estimated values by noise. In cases where the evaluation threshold was not supported by an APDP of at least one band, the data of all bands was discarded for the comparison.

Figure 1 shows the empirical cumulative distribution functions (CDFs) of the DS for three different thresholds, namely 15, 20 and 25 dB at a Tx-Rx distance of up to 110 m. These are based on 3000 APDPs for each frequency band. As expected, increasing the threshold yields higher values and the CDFs shift to the right. The results for the three frequencies are very similar for $\Gamma = 15$dB and $\Gamma = 20$ dB. There is only a small trend towards larger spreads for 10 GHz, which occurs with lower probability. However, for $\Gamma = 25$ dB this trend becomes more distinct, whereas the curves for 28.5 and 41.5 GHz are still practically congruent.

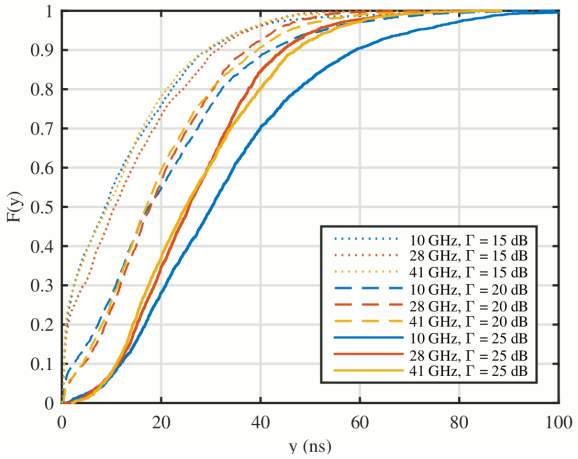

Figure 1. Empirical CDFs of RMS delay spread for 10–110 m distance range and relative thresholds of 15, 20 and 25 dB.

Results on the comparison of all four frequencies are illustrated in Figure 2. In this case, a threshold of 15 dB was chosen and the evaluated distance range was limited to 10–60 m. Compared to the results based on the distance range 10–110 m lower DSs occur with higher probability. The CDFs are less smooth as only 600 APDPs for each frequency are available that exhibit the required dynamic range at the respective Rx position for each measured band (after bandwidth limitation of the upper bands), including 82 GHz. The DS for 82 GHz is clearly smaller than for the lower bands. However, for the lower bands a trend of a potential frequency dependence cannot be identified based on this subset of data samples. Figure 2 shows that the considered distance range can impact the results and that a large sample size is beneficial to enable clear conclusions. Preliminary investigations on the dependence of the DS on Tx-Rx distance indicate that lower values and lower variations occur for very small distances (10–20 m). Both tend to increase with distance, but saturate at distances between 30 and 50 m.

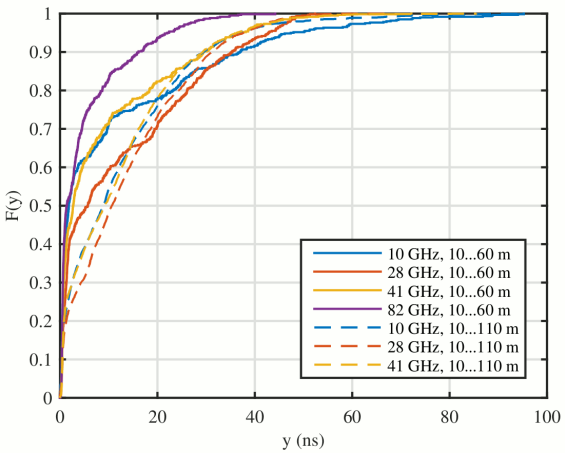

Figure 2. Empirical CDFs of RMS delay spread for 10–60 m Tx-Rx distance and relative threshold of 15 dB.

5. Conclusion

An initial statistical analysis of the DS based on LOS data of a multi-frequency channel measurement campaign in an UMi street canyon scenario has been presented. In order to ensure the greatest comparability, the data for the higher bands was reduced to the same bandwidth as used for 10.25 GHz, namely 500 MHz. The same relative evaluation threshold was applied to the power delay profiles for all bands. Based on the data for distances between 10 and 110 m, it can be shown that the distribution of the DS for the lower bands (10, 28, 41 GHz) is very similar for evaluation thresholds of 15 and 20 dB. For a threshold of 25 dB, there is a trend to higher values for 10 GHz. A statistical analysis based on a reduced data set for the distance range 10–60 m shows that the DS is tendentially lower at 82 GHz in comparison to the other frequencies. However, taking into account all results, a distinct and clear frequency dependence cannot be identified. In conjunction with findings in the literature, these results indicate that the frequency dependence is scenario-specific and may e.g. differ for indoor and outdoor environments.

Acknowledgment

The research leading to these results received funding from the European Commission H2020 programme under grant agreement n°671650 (5G PPP mmMAGIC project).

References

[1] F. Boccardi, R. Heath, A. Lozano, T. Marzetta, and P. Popovski, "Five disruptive technology directions for 5G," Communications Magazine, IEEE, vol. 52, no. 2, pp. 74–80, 2014.

[2] ICT-671650 mmMAGIC D2.1, "Measurement Campaigns and Initial Channel Models for Preferred Suitable Frequency Ranges," Mar. 2016.

[3] 3GPP TR 36.873 V12.2.0, "Study on 3D channel model for LTE," Tech.Rep., 2015.

[4] ICT-317669 METIS D1.4, "METIS Channel Models," Jul. 2015.

[5] S. Jaeckel, L. Raschkowski, K. B¨orner, and L. Thiele, "QuaDRiGa: A 3-D Multi-Cell Channel Model with Time Evolution for Enabling Virtual Field Trials," IEEE Trans. Antennas Propag., vol. 62, pp. 3242–3256, 2014.

[6] ITU-R P.1411-8, "Propagation data and prediction methods for the planning of short-range outdoor radiocommunication systems and radio local area networks in the frequency range 300 MHz to 100 GHz," Tech. Rep., 2015.